Doctoral Dissertation

Hormonal mechanisms in the paraventricular nuclei associated with hyperalgesia in Parkinson's disease model rats

パーキンソン病モデルラットにおける室傍核のホルモン機構と痛覚過敏の関連性

Osaka University Graduate School of Dentistry

Course for Oral Science

(Department of Dental Anesthesiology)

Shengsen Yang

Publication and Presentations

This dissertation includes research findings that have been published in an academic journal and presented at academic conferences. The details are as follows:

Journal Publication

S. Yang, N. Usami, S. Lu, W. Oda, H. Maegawa, H. Niwa, C. Kudo,
Hormonal mechanisms in the paraventricular nuclei associated with hyperalgesia in Parkinson's disease model rats.
Biochemical and Biophysical Research Communications (2024), Article 151178.
https://doi.org/10.1016/j.bbrc.2024.151178

Conference Presentations

1. **The 14th Annual Meeting of the Federation of Asian Dental Anesthesiology Societies**
Nagasaki International Exhibition Hall, Nagasaki, Japan, October 2023

2. **Oral Neuroscience 2023**
Osaka University Graduate School of Dentistry, Osaka, Japan, April 2024

Index

1. List of Abbreviations

PD: Parkinson's disease

QOL: quality of life

PVN: paraventricular nucleus

6-OHDA: 6-hydroxydopamine

OXT: oxytocin

AVP: arginine vasopressin

CRH: corticotropin-releasing hormone

-IR: -immunoreactive

Vc: trigeminal spinal subnucleus caudalis

SC: subcutaneous

IP: intraperitoneal

MFB: medial forebrain bundle

TH: tyrosine hydroxylase

p-ERK: phosphorylated extracellular signal-regulated kinase

RT: room temperature

2. Introduction

Parkinson's disease (PD) is a chronic, progressive neurodegenerative disorder characterized by the loss of dopaminergic neurons in the substantia nigra pars compacta and the formation of α-synuclein aggregates [1,2]. The main clinical manifestations of PD are motor symptoms including bradykinesia, resting tremor, muscle tonus and postural instability, which significantly affect mobility and daily functioning [3-5]. In addition to motor symptoms, PD is accompanied by a variety of non-motor symptoms, including cognitive decline, mood disorders (e.g., depression and anxiety), autonomic dysfunction, sleep disturbances, and sensory abnormalities [6,7]. Pain is a common but often overlooked non-motor symptom, and PD patients complain of a variety of pain types, including musculoskeletal pain, neuropathic pain, dystonia-related pain, and central pain [8]. These pain experiences can interfere with daily activities, disrupt sleep, and lead to emotional distress and social isolation [9].

Hyperalgesia is a common nonmotor symptom in PD patients that significantly affects the quality of life (QOL) [1,10-14]. Previous studies using skin electrical pulse stimulation have demonstrated that patients with Parkinson's disease have significantly lower pain thresholds and pain tolerance compared to controls, along with the presence of hyperalgesia [15]. In line with this heightened pain sensitivity, PD patients are also more likely than the general population to experience oral pain or suffer from burning mouth syndrome [16,17]. Notably, 24% of patients with Parkinson's disease have burning mouth syndrome, a rate five times higher than that of the controls [18]. Recent studies have demonstrated that hyperalgesia in PD patients is mainly associated with

pathological changes in the central nervous system, including the loss of dopaminergic neurons and alterations in pain modulation pathways [14,19]. More than half of PD patients report chronic pain, including spontaneous pain and hyperalgesia, which severely impact their QOL and are often clinically overlooked, leading to inadequate management and treatment [1,11,13,14,20]. Therefore, understanding the mechanisms underlying hyperalgesia in PD is crucial.

In PD model rats, unilateral or bilateral injections of 6-hydroxydopamine (6-OHDA) into the medial forebrain bundle (MFB) have been reported to cause hyperalgesia [10-12,14]. Several reports have suggested that altered neuronal activity in the paraventricular nucleus (PVN) is associated with hyperalgesia in rat models of PD induced by 6-OHDA injection (6-OHDA rats) [14,21]. We previously demonstrated that the subcutaneous (SC) injection of formalin into the vibrissa pad of 6-OHDA rats increased face-rubbing behavior and the number of c-Fos-immunoreactive (c-Fos-IR) cells in the trigeminal spinal subnucleus caudalis (Vc), indicating hyperalgesia in 6-OHDA rats [11,12,14]. Furthermore, the SC injection of formalin into the vibrissa pad increased the neuronal activity of oxytocin (OXT) in the PVN and blood OXT levels in sham rats but suppressed them in 6-OHDA rats [14]. We also reported that intracisternal administration of OXT alleviated hyperalgesia in 6-OHDA rats. These findings suggest that hyperalgesia in 6-OHDA rats can be caused by the suppression of the analgesic effect of OXT originating from the PVN [12,14].

The PVN contains neurosecretory cells that produce OXT, arginine vasopressin (AVP), and corticotropin-releasing hormone (CRH) [22,23]. OXT has already been investigated in relation to hyperalgesia in 6-OHDA rats [14], but AVP and CRH have not been examined yet [24,25]. Previous studies have shown that the function of the

PVN is decreased in PD patients [14], suggesting that all hormones synthesized and secreted by the PVN may be altered in PD patients. As Both OXT and CRH have been shown to be associated with pain responses [22,23], whereas AVP and CRH are associated with stress responses [24,25], the mechanisms of hyperalgesia in PD may be revealed by applying nociceptive stimuli to PD model rats and examining the OXT, AVP and CRH responses to them. The present study aimed to investigate the immunohistochemical responses in OXT, AVP, and CRH cells in the PVN and the changes in the serum levels of these neuropeptides following nociceptive stimulation in PD model rats, and to understand the mechanisms underlying hyperalgesia in PD.

3. Materials and Methods

3.1 Animals

A total of 47 male Wistar rats (Japan SLC, Inc., Shizuoka, Japan; weight: 150–200 g) were used in this study. The rats were housed under a 12-h dark/light cycle and provided access to food and water ad libitum. The study was approved by the Animal Care and Use Committee of Osaka University Graduate School of Dentistry (Approval No. R-03-002-0), and all experimental procedures were performed according to the National Institute of Health Guide for the Care and Use of Laboratory Animals.

3.2 Induction of 6-OHDA lesions

Of the 47 rats, 35 rats underwent induction of PD models, as previously reported [11,12,14]. Rats were anesthetized intraperitoneally (IP) with a saline solution containing midazolam (2.0 mg/kg, Sandoz, Tokyo, Japan), medetomidine (0.375 mg/kg, Zenoaq, Fukushima, Japan) and butorphanol (2.5 mg/kg, Meiji Seika Pharma, Tokyo, Japan), and placed in a stereotaxic apparatus (SR-6, Narishige, Tokyo, Japan). A burr hole was drilled over the skull, and unilateral nigrostriatal lesions were created by injecting 6-OHDA (Sigma, St. Louis, MO, USA; 15 μg in 5 μL of sterile saline containing 0.01% ascorbic acid) into the left MFB. The stereotaxic coordinates of the lesions were 3.3 mm rostral to the interaural line, 1.4 mm left of the midline, and 6.8 and 6.5 mm ventral to the dural surface (2.5 μL injected to each location). The 6-OHDA solution was administered through a cannula using a microinjection pump (KDS-100, Nihon Kohden, Tokyo, Japan) at a rate of 1 μL/min. The cannula was left in place for 5

min after the completion of each injection, then the hole was covered with the bone wax. Twelve rats were assigned to the sham rats, underwent the same surgical procedures, and received an injection of sterile saline solution containing 0.01% ascorbic acid into the same coordinates as the 6-OHDA rats, with the saline injected in the same volume and at the same rate as the 6-OHDA solution. The cannula was similarly left in place for 5 min, and the burr hole was closed with bone wax after injection.

3.3 Rotational behavior test

Two weeks after 6-OHDA or saline administration into the left MFB, the rats were placed in a cylindrical container (300 mm in diameter), and IP administration of methamphetamine (3 mg/kg, Sumitomo Pharma, Osaka, Japan) was performed to trigger rotational behavior [26]. The frequency of the behavior was recorded using a video camera over 1 hour after the methamphetamine administration, and animals exhibiting a total of ≥ 300 turns within 1 hour were identified as 6-OHDA rats [27]. In contrast to 6-OHDA rats, the sham rats did not exhibit any rotational behavior by the methamphetamine administration.

3.4 Formalin SC injection

Because the neuronal activity in the PVN exhibits circadian rhythmicity, all experiments were performed between 9 AM and 3 PM to minimize the influence of diurnal variations [28].

Rats were randomly divided into two groups according to the SC injection stimulation: saline-injected groups or formalin-injected groups. Three weeks after 6-OHDA or saline administration into the left MFB, the rats were anesthetized using the IP injection of sodium pentobarbital (50 mg/kg). The depth of anesthesia was confirmed by assessing the loss of the righting reflex [29]. Once adequate anesthesia was achieved, the rats received a 50-µl SC injection of saline or 4% formalin dissolved in saline into the vibrissa pad on the same side of MFB administration using a 26-gauge needle [11,12,14].

3.5 Enzyme immunoassay for OXT, AVP, and CRH in serum

Five minutes after the SC injection, the rats were anesthetized with an IP overdose of sodium pentobarbital (120 mg/kg). Subsequently, 3.0 mL of blood was collected from their hearts. The collected blood samples were centrifuged at 4°C and 1600×g for 15 min (KITMAN-18, TOMY DIGITAL BIOLOGY, Tokyo, Japan). The serum samples were collected and stored in aliquots at −70°C until analysis. The serum concentrations of OXT, AVP and CRH were analyzed using specific enzyme immunoassay kits (OXT: ADI-900-153A-0001, Enzo Life Science Inc., NY, USA, AVP: ADI-900-017A, Enzo Life Science Inc., CRH: CEA835RA, CLOUD-CLONE CORP., TX, USA). All serum samples were thawed only once before use and underwent a preliminary experiment before the formal trial to ensure that the sample concentrations were within the measurement range. Luminescence counts were measured using a iMark™ Microplate Absorbance Spectrophotometer (Bio-Rad Laboratories Inc., CA, USA).

3.6 Histology

Immediately after the blood collection from the rats, intracardial perfusion was performed using 150 mL of phosphate-buffered saline (PBS, 0.02 M, pH 7.4), followed by 500 mL of 4% (w/v) paraformaldehyde in PBS. The brain was then removed, post-fixed at 4°C for 24 h, and transferred to 30% sucrose in 0.01 M PBS at 4°C for 48 h. Serial coronal sections were created using a freezing microtome at 40-μm thickness, and all sections were stored in PBS.

3.7 Tyrosine hydroxylase (TH) immunohistochemistry

6-OHDA rats were evaluated using the methamphetamine-induced rotational behavior test and immunoreactivity for TH, which is a dopaminergic neuron marker, to characterize the PD model in all experiments.

The sections containing the striatum and substantia nigra pars compacta were incubated with 0.3% hydrogen peroxide in methanol for 20 min and then rinsed three times with PBS for 5 min each. The sections were blocked with 1% normal horse serum (NHS, Vector Labs, Burlingame, CA, USA) and 0.1% Triton X-100 in PBS for 30 min at room temperature (RT). The sections were then incubated with mouse anti-TH antibody (1:8000, T2928, Sigma-Aldrich, St. Louise, MO, USA), 1% NHS and 0.1% Triton X-100 in PBS overnight at 4°C. The sections were then rinsed three times with PBS for 5 min each and incubated with a biotinylated horse anti-mouse antibody (1:200, Vector Labs, Burlingame, CA, USA) for 1 h at RT. The sections were then rinsed three times with PBS for 5 min each and incubated with the avidin-biotin-peroxidase complex (1:200, ABC Elite kit, Vector Labs) for 1 h. The sections were finally treated with a

DAB Substrate kit (Sigma-Aldrich), mounted on glass slides, air-dried, dehydrated, and cover-slipped [11,12,14].

3.8 p-ERK immunohistochemistry in the Vc

To determine whether 6-OHDA rats experienced hyperalgesia after the SC injection of formalin, immunoreactivity analyses for p-ERK (a marker of activated neuronal nuclei) in the Vc were performed.

The sections containing Vc were incubated with 0.3% hydrogen peroxide in methanol for 20 min and then rinsed three times with PBS for 5 min each. The sections were blocked with 1% NHS and 0.1% Triton X-100 in PBS for 30 min at RT. The sections were then incubated with mouse anti-p-ERK antibody (1:500, sc-136521, Santa Cruz Biotechnology, Dallas, Texas USA), 1% NHS and 0.1% Triton X-100 in PBS overnight at 4°C. The sections were then rinsed three times with PBS for 5 min each and incubated with a biotinylated horse anti-mouse antibody (1:200, Vector Labs) for 1 h at RT. The sections were then rinsed three times with PBS for 5 min each and incubated with the avidin-biotin-peroxidase complex (1:200, ABC Elite kit) for 1 h. The sections were finally treated with a DAB Substrate kit, mounted on glass slides, air-dried, dehydrated, and cover-slipped [11,12,14].

3.9 Double immunofluorescence in the PVN

Double immunofluorescent labeling for p-ERK/OXT, p-ERK/AVP, and p-ERK/CRH in the sections containing the PVN was achieved by incubating the sections with specific primary antibodies [14]. The sections were blocked with 10% NGS and 0.3% Triton X-100 in PBS for 1 h at RT. The sections were then incubated overnight at 4℃ with three patterns of primary antibodies, 2% NGS, and 0.3% Triton X-100 in PBS; a mixture of rabbit anti-OXT antibody (1:1000, MAB5296, Merck Millipore, Burlington, MA, USA) and mouse anti-p-ERK antibody (1:200, sc-136521) for the first pattern; a mixture of rabbit anti-AVP antibody (1:1000, AB1565, Merck Millipore) and mouse anti-p-ERK antibody (1:200, sc-136521) for the second pattern; and a mixture of rabbit anti-CRH antibody (1:500, C5348, Sigma-Aldrich) and mouse anti-p-ERK antibody (1:200, sc-136521) for the third pattern. The sections were then rinsed three times with PBS for 5 min each and incubated with secondary antibodies, which are a mixture of goat anti-rabbit Alexa Fluor 488 (1:200, Invitrogen, Carlsbad, CA, USA), goat anti-mouse Alexa Fluor 568 (1:200, Invitrogen) and 2% NGS in PBS for 2 h at RT. The sections were rinsed three times with PBS for 5 min each, mounted on glass slides, and cover-slipped. The negative control sections confirmed the specificity of staining because the omission of primary antibodies resulted in no detectable labeling.

3.10 Cell counting

The anatomical locations within the Vc and PVN were identified using the Paxinos and Watson atlas [30]. Images were obtained using a light microscope (BX51, Olympus, Tokyo, Japan) or a confocal laser microscope (TCS SP8, Leica Microsystems, Wetzlar,

Germany) at 10× magnification. In each rat, cells were counted in five sections in the Vc and three sections in the PVN, following established methods [11,12,14]. The number of cells was counted by one examiner who was blinded to the experimental procedures.

To quantify the proportion of OXT, AVP, and CRH neurons activated by the SC injection of formalin into the vibrissa pad, the percentage of OXT-IR, AVP-IR, and CRH-IR neurons expressing p-ERK protein in the PVN was calculated using the following formula [14]:

$$\left(\frac{\text{Nmber of OXT-, AVP-, or CRH-IR neurons co-localized with p-ERK protein}}{\text{Nmber of OXT-, AVP-, or CRH-IR neurons}}\right) \times 100\ (\%)$$

3.11 Statistical analyses

Data are expressed as mean ± standard error of the mean. All experimental results were analyzed using two-way analysis of variance (ANOVA), followed by Bonferroni's post-hoc test for multiple comparisons where relevant. All statistical analyses were performed using SPSS (IBM, Statistics ver. 24, IL, USA), and *p-value* < 0.05 was considered statistically significant.

4. Results

4.1 Rotational behavior distribution of 6-OHDA-injected rats

The rotational behavior test of 35 rats injected with 6-OHDA was assessed two weeks after the injection to evaluate the success of the PD model. The number of rotations per hour was categorized into four groups: ≤100, 101–200, 201–300, and >300 rotations/hour (Fig .1). 12 of the 35 rats rotated more than 300 times per hour and were used as 6-OHDA rats, while the remaining 23 rats were excluded.

4.2 TH immunoreactivity

TH immunohistochemical staining was performed on all rats to confirm dopamine depletion by unilateral 6-OHDA administration into the MFB. The sham rats exhibited high TH immunoreactivity in the striatum and substantia nigra on both sides [Fig. 2 (a and b)]. Contrarily, the 6-OHDA rats showed a significant decrease in TH immunoreactivity in the striatum and substantia nigra on the same side of 6-OHDA administration [Fig. 2 (c and d)].

4.3 p-ERK expression in the Vc

Immunohistochemical staining for p-ERK in the Vc (Fig. 3A) was performed, and the number of p-ERK-IR cells in the superficial layers of the Vc was counted. The

number of p-ERK-IR cells in the Vc was analyzed using two-way ANOVA with factors of group (sham vs. 6-OHDA) and treatment (saline vs. formalin). The results revealed no significant group effect [F(1,20) = 2.6, n=6 each, *p-value* = 0.12], a significant treatment effect [F (1,20) = 40.8, n=6 each, *p-value* < 0.001], and a significant interaction effect [F (1,20) = 5.4, n=6 each, *p-value* = 0.03].

Post-hoc Bonferroni test showed that in the sham rats, the number of p-ERK-IR cells in the formalin-injected group was significantly higher than that in the saline-injected group [F (1,20) = 8.2, n=6 each, *p-value* = 0.009; Fig. 3B]. In the formalin-injected groups, the 6-OHDA rats exhibited a significant increase in p-ERK-IR cells compared to the sham rats [F (1,20) = 7.8, n=6 each, *p-value* = 0.011; Fig. 3B]. Moreover, in the 6-OHDA rats, the number of p-ERK-IR cells in the formalin-injected group was significantly higher than that in the saline-injected group [F (1,20) = 38.0, n=6 each, *p-value* < 0.001; Fig. 3B].

4.4 p-ERK expression in the PVN

Fluorescent double staining of OXT, CRH, AVP-IR and p-ERK-IR cells in the PVN was performed. Two-way ANOVA showed a significant group effect [F (1,20) = 14.0, n=6 each, *p-value* = 0.001], a significant treatment effect [F (1,20) = 23.6, n=6 each, *p-value* < 0.001], and a significant interaction effect [F (1,20) = 8.8, n=6 each, *p-value* = 0.008].

Post-hoc Bonferroni test revealed that in the sham rats, the number of p-ERK-IR Cells in the PVN was significantly higher in the formalin-injected group than in the saline-injected group [F (1,20) = 30.5, n=6 each, *p-value* < 0.001; Fig. 4]. In the 6-

OHDA rats, no significant difference was observed between the two groups [F (1,20) = 1.8, n=6 each, *p-value* = 0.19; Fig. 4]. Moreover, in the formalin-injected group, the number of p-ERK-IR Cells in the PVN was significantly lower in the 6-OHDA rats than in the sham rats [F (1,20) = 22.4, n=6 each, *p-value* < 0.001; Fig. 4]

4.5 Co-expression of p-ERK and OXT in the PVN

Fluorescent double staining of OXT-IR and p-ERK-IR cells in the PVN was performed (Fig. 5A, p-ERK-IR cells: a-d, OXT-IR cells: e-h, merged images: i-l). Two-way ANOVA showed a significant group effect [F (1,20) = 6.4, n=6 each, *p-value* = 0.02], a significant treatment effect [F (1,20) = 8.7, n=6 each, *p-value* = 0.008], and a significant interaction effect [F (1,20) = 11.1, n=6 each, *p-value* = 0.003].

Post-hoc Bonferroni test showed that in the sham rats, the percentage of OXT-IR neurons co-localized with p-ERK protein in the PVN was significantly higher in the formalin-injected group than in the saline-injected group [F (1,20) = 19.7, n=6 each, *p-value* < 0.001; Fig. 5B], whereas, in the 6-OHDA rats, no significant difference was observed between the two groups [F (1,20) = 0.08, n=6 each, *p-value* = 0.8; Fig. 5B]. Moreover, in the formalin-injected group, the percentage of OXT-IR neurons co-localized with p-ERK protein in the PVN was significantly lower in the 6-OHDA rats than in the sham rats [F (1,20) = 17.2, n=6 each, *p-value* < 0.001; Fig. 5B].

4.6 Co-expression of p-ERK and CRH in the PVN

Fluorescent double staining of CRH-IR and p-ERK-IR cells in the PVN was performed (Fig. 6A, p-ERK-IR cells: a-d, CRH-IR cells: e-h, merged images: i-l). Two-

way ANOVA showed a significant group effect [F (1,20) = 22.1, n=6 each, *p-value* < 0.001], a significant treatment effect [F (1,20) = 9.7, n=6 each, *p-value* = 0.006], and a significant interaction effect [F (1,20) = 5.0, n=6 each, *p-value* = 0.04].

Post-hoc Bonferroni test showed that in the sham rats, the percentage of CRH-IR neurons co-localized with p-ERK protein in the PVN was significantly higher in the formalin-injected group than in the saline-injected group [F (1,20) = 14.3, n=6 each, *p-value* = 0.001; Fig. 6B], whereas, in the 6-OHDA rats, no significant difference was observed between saline- and formalin-injected groups [F (1,20) = 0.4, n=6 each, *p-value* = 0.5; Fig. 6B]. In the formalin-injected group, the percentage of CRH-IR neurons co-localized with p-ERK protein in the PVN was significantly lower in the 6-OHDA rats than in the sham rats [F (1,20) = 24.1, n=6 each, *p-value* < 0.001; Fig. 6B].

4.7 Co-expression of p-ERK and AVP in the PVN

Fluorescent double staining of AVP-IR and p-ERK-IR cells in the PVN was performed (Fig. 7A, p-ERK-IR cells: a-d, AVP-IR cells: e-h, merged images: i-l). Two-way ANOVA showed a significant group effect [F (1,20) = 188.1, n=6 each, *p-value* < 0.001], no significant treatment effect [F (1,20) = 3.5, n=6 each, *p-value* = 0.08], and no significant interaction effect [F (1,20) = 1.1, n=6 each, *p-value* = 0.3].

Post-hoc Bonferroni test showed that in both the saline- and formalin-injected groups, the percentage of AVP-IR neurons co-localized with p-ERK protein was significantly lower in the 6-OHDA rats than in the sham rats [saline-injected group: F (1,20) = 109.3, n=6 each, *p-value* < 0.001; formalin-injected group: F (1,20) = 80.0, n=6 each, *p-value* < 0.001; Fig. 7B]. In both the sham and 6-OHDA rats, no significant

difference was observed between the saline- and formalin-injected groups [sham rats: F (1,20) = 0.3, n=6 each, *p-value* = 0.6; 6-OHDA rats: F (1,20) = 4.3, n=6 each, *p-value* = 0.06; Fig. 7B]

4.8 Effect of SC formalin injection on serum OXT concentration

Two-way ANOVA showed a significant group effect [F (1,20) = 8.4, n=6 each, p-value = 0.009], no significant treatment effect [F (1,20) = 1.5, n=6 each, *p-value* = 0.2], and a significant interaction effect [F (1,20) = 5.8, n=6 each, *p-value* = 0.03].

Post-hoc Bonferroni test showed that in the sham rats, the serum OXT concentration was significantly higher in the formalin-injected group than in the saline-injected group [F (1,20) = 6.6, n=6 each, *p-value* = 0.02, Fig. 8A]. Conversely, in the 6-OHDA rats, no significant difference in serum OXT concentration was observed between the saline- and formalin-injected groups [F (1,20) = 0.72, n=6 each, *p-value* = 0.4, Fig. 8A]. Moreover, in the formalin-injected group, the serum OXT concentration was lower in the 6-OHDA rats than in the sham rats [F (1,20) = 14.1, n=6 each, *p-value* = 0.001; Fig. 8A].

4.9 Effect of SC formalin injection on serum CRH concentration

Two-way ANOVA showed a significant group effect [F (1,20) = 7.5, n=6 each, p-value = 0.01], a significant treatment effect [F (1,20) = 5.9, n=6 each, *p-value* = 0.03], and a significant interaction effect [F (1,20) = 14.2, n=6 each, *p-value* = 0.001].

Post-hoc Bonferroni test showed that in the sham rats, the serum CRH concentration was significantly higher in the formalin-injected group than in the saline-injected group [F (1,20) = 19.3, n=6 each, *p-value* < 0.001, Fig. 8B]. Conversely, in the 6-OHDA rats, no significant difference in serum CRH concentration was observed between the saline- and formalin-injected groups [F (1,20) = 0.9, n=6 each, *p-value* = 0.4, Fig. 8B]. In the formalin-injected group, the serum CRH concentration was significantly lower in the 6-OHDA rats than in the sham rats [F (1,20) = 21.2, n=6 each, *p-value* < 0.001, Fig. 8B]

4.10 Effect of SC formalin injection on serum AVP concentration

Two-way ANOVA showed a significant group effect [F (1,20) = 29.2, n=6 each, p-value < 0.001], no significant treatment effect [F (1,20) = 1.8, n=6 each, *p-value* = 0.2], and no significant interaction effect [F (1,20) = 0.08, n=6 each, *p-value* = 0.9].

Post-hoc Bonferroni test showed that in both the saline- and formalin-injected groups, the serum AVP concentration was significantly lower in the 6-OHDA rats than in the sham rats [saline-injected group: F (1,20) = 14.6, n=6 each, *p-value* = 0.001; formalin-injected group: F (1,20) = 14.6, n=6 each, *p-value* = 0.001, Fig. 8C]. In both the sham and 6-OHDA rats, no significant difference was observed between the saline- and formalin-injected groups [sham rats: F (1,20) = 0.9, n=6 each, *p-value* = 0.4; 6-OHDA rats: F (1,20) = 0.9, n=6 each, *p-value* = 0.4; Fig. 8C].

5. Discussion

OXT, AVP, and CRH are the neuropeptides known to be synthesized in the PVN [22,23,31]. Both OXT and CRH exhibit analgesic effects and are enhanced by neuronal activity; their synthesis and secretion are also promoted by nociceptive stimuli [14,32]. In this study, nociceptive stimuli enhanced the neuronal activity of producing cells and increased serum OXT and CRH levels in sham rats. In contrast, the enhancement in neuronal activity and the increase in serum OXT and CRH levels were suppressed in 6-OHDA rats. This suggests that the synthesis and secretion of OXT and CRH promoted by nociceptive stimuli are suppressed in 6-OHDA rats, potentially leading to reduced analgesic effects of OXT and CRH, thereby resulting in hyperalgesia. However, no changes in serum AVP concentrations or neuronal activity were observed in response to nociceptive stimuli in either the sham or 6-OHDA group. This suggests that AVP is unaffected by nociceptive stimuli and is not involved in PD-associated hyperalgesia.

The decision to collect the blood samples at five minutes after formalin injection (early phase) rather than at a later time point (late phase) had two reasons: one was the nociceptive properties of formalin injection and the other was the half-life of the hormone in the blood. The pain response triggered by formalin injections is divided into two main phases: early phase and late phase. The early phase usually occurs in the first 5 minutes after injection and is driven by immediate neuroreflexes and activation of primary sensory neurons [33,34]. The pain response in this phase is closely related to the immediate excitation of nociceptors, reflecting the immediate effect of the painful stimulus and allowing a more realistic assessment of the acute effects of nociceptive

stimuli on neurohormone release [35]. In addition, the half-life of these hormones in the blood of rats is typically only a few minutes. For example, it has been shown that OXT has a half-life in plasma of approximately 1-3 minutes [36]. Due to the rapid degradation of hormones, blood collection at later time points may not accurately reflect the initial effects of the pain stimulus, but rather confound the results of compensatory feedback mechanisms, thereby compromising the reliability of the data.

Various theories regarding the analgesic mechanism of OXT have been proposed. OXT exerts analgesic effects by stimulating the descending pain modulation pathways in the spinal cord and brainstem, particularly through its interactions with the periaqueductal gray and locus coeruleus regions [14,37,38]. This activation promotes the release of opioids within these areas, thereby inhibiting pain transmission [39-42]. Furthermore, OXT enhances the analgesic effects by promoting the release of endogenous opioid peptides, such as β-endorphins [41]. OXT also reduces inflammatory responses, alleviating inflammation-related pain, which is associated with the inhibition of pro-inflammatory factors, such as tumor necrosis factor-alpha and interleukin-6 [38,39]. Moreover, OXT influences pain perception by modulating the brain regions associated with emotional processing, including the prefrontal cortex and amygdala.

CRH plays a key role in the body's response to stress by activating the hypothalamic-pituitary-adrenal axis, which leads to the release of glucocorticoids [24,25]. These glucocorticoids alleviate pain by reducing inflammation and increasing pain tolerance, which is a mechanism often referred to as stress-induced analgesia [25,32]. Additionally, CRH modulates the endogenous opioid system and activates the descending pain pathways, thereby enhancing pain inhibition [32,42]. Furthermore, although CRH reduces pain during acute stress, the prolonged release of CRH during

chronic stress may actually increase pain perception [24,43]. This dual effect highlights the complex role of CRH in the nervous system, where it can either promote or inhibit pain, depending on the duration and context of the stress [24,43]. To confirm the involvement of suppressed OXT and CRH synthesis or secretion in PD-related hyperalgesia, behavioral experiments involving OXT and CRH administration are necessary.

In response to nociceptive stimuli, the synthesis and secretion pathways of OXT and CRH involve rapid neuroendocrine responses [44,45]. Pain signals are transmitted to the central nervous system (CNS) through the dorsal horn of the spinal cord and tracts, and upon reaching the medulla oblongata, A1/A2 noradrenergic neurons are activated and release noradrenaline (NA) [46,49]. NA sends excitatory signals to OXT and CRH neurons located in the PVN and supraoptic nucleus, thereby precipitating the release of these hormones [50,51]. OXT is transported via axons to the posterior pituitary gland, where it is released into the peripheral blood and locally in the CNS to modulate pain and emotional responses [52,53]. CRH is transported to the median eminence and secreted into the hypothalamo-pituitary portal system, where it stimulates the anterior pituitary gland to release adrenocorticotropic hormone, which in turn activates the hypothalamo-pituitary-adrenal axis, resulting in a systemic stress response [45,51,54-56]. This sequence of events ensures that OXT and CRH are rapidly secreted following nociceptive stimulation, resulting in the timely modulation of pain and stress responses [55,57].

The suppression of the neural activation of OXT and CRH in 6-OHDA rats may be attributed to changes in the dopaminergic or noradrenergic neuronal systems. The degeneration of dopaminergic neurons induced by 6-OHDA may alter dopamine

projections to the PVN [31,46]. Furthermore, 6-OHDA may affect noradrenergic projections from the A1/A2 cell groups to the PVN [46,47]. In the creation of rat models of PD, desipramine, a noradrenaline reuptake inhibitor, is sometimes administered IP before 6-OHDA administration to denervate only dopaminergic neurons [58]. However, it has been reported that the 6-OHDA-induced damage to NA neurons cannot be fully blocked by desipramine [59]. Furthermore, in PD patients, degeneration is not limited to the dopaminergic system; the NA system also exhibits significant neurodegenerative changes [60]. Therefore, the dual dysfunction of the dopaminergic and noradrenergic systems may collectively contribute to the suppression of OXT and CRH neural activation within the PVN, leading to the hyperalgesia observed in the rat models of PD.

The expression of receptors related to pain modulation, particularly the oxytocin receptor (OXTR) and CRH receptor (CRHR), in the trigeminal ganglion (TG) and Vc has been addressed in several studies. OXT exerts analgesic effects on the spinal cord and brainstem regions through the activation of descending pain inhibitory pathways, including modulation of the OXTR in the TG [61-63]. In addition, OXT acts directly on the OXTR in the TG to alleviate migraine-associated pain [64]. Although chronic pain causes the upregulation of OXTR expression in the TG [61], the mechanism through which formalin stimulation alters OXTR expression in the Vc or TG remains unclear. Similarly, the CRHR is widely distributed in the central and peripheral nervous systems, and it is involved in pain modulation and stress responses [65]. Although CRHR expression in brainstem regions has been confirmed [65,66], changes in CRHR expression in the Vc or TG have not been definitively established. Inflammatory mediators may affect CRHR expression, and CRHR expression may be altered under

chronic pain conditions [67,68]. Overall, the potential roles of these receptors in pain signaling warrant further investigation.

PD patients have low AVP levels, which tend to cause urinary incontinence [69,70]. This decrease is considered to be caused by the renin–angiotensin (AT)–aldosterone system, which regulates AVP synthesis and release [61]. AT receptors have three subtypes in the brain, with the AT1 receptor being predominantly distributed in the striatum and substantia nigra, which control AVP release [21]. In PD patients , damage to the striatum and substantia nigra affects the function of the AT1 receptor, thereby influencing AVP synthesis and secretion [21]. In this study, the neuronal activity and serum concentration of AVP did not change in response to noxious stimuli in either sham or 6-OHDA rats, and they consistently remained lower in 6-OHDA rats. These findings are consistent with those of previous studies that reported low AVP levels in PD patients [69], suggesting that AVP does not directly affect hyperalgesia in rats with PD. Considering that AVP receptors exert analgesic effects in coordination with opioids and CRH [71], reduced AVP levels in rats with PD may lead to alterations in AVP receptors, potentially affecting analgesic pathways. However, further research is necessary to investigate changes in AVP receptors in rats with PD.

The etiology of PD-related pain is complex and can be categorized into musculoskeletal, neuropathic, dystonia-related, and central pain. Effective pain management requires a comprehensive consideration of pain type, underlying mechanisms, and individual differences [72]. For pain management in PD patients, optimizing antiparkinsonian therapy is fundamental, such as adjusting the dosage of levodopa or dopamine agonists (e.g., rotigotine and safinamide), which can alleviate pain associated with motor symptoms [73,74]. Furthermore, nonsteroidal anti-

inflammatory drugs (e.g., ibuprofen and diclofenac) are commonly used to manage musculoskeletal pain, opioids (e.g., oxycodone/naloxone extended-release tablets) are effective for managing central and refractory pain [72,75], and drugs such as gabapentin and pregabalin are indicated for neuropathic pain [76]. However, these conventional pain treatments do not specifically target hyperalgesia and often come with side effects such as nausea, drowsiness, and dizziness. This study demonstrated that OXT and CRH responses to nociceptive stimuli were significantly suppressed in PD rats, suggesting that the dysfunction of these neuropeptides contributes to pain sensitization in PD. Given their known analgesic properties, restoring OXT and CRH function may be a potential therapeutic strategy for managing PD-related hyperalgesia. Although no clinically approved OXT- or CRH-based treatments currently exist, further research into neuropeptide modulation, receptor agonists, or delivery methods may facilitate drug development for hyperalgesia management and provide new insights into alternative pain treatment strategies.

6. Conclusion

The enhanced neuronal activity and increased serum concentrations of OXT and CRH in response to nociceptive stimuli were suppressed in PD rats. These findings suggest that the reduced analgesic effects of OXT and CRH in response to nociceptive stimuli may contribute to hyperalgesia in PD rats. Our data could shed light on the mechanisms underlying hyperalgesia in PD and potentially form the basis for future treatments to alleviate hyperalgesia.

7. Acknowledgment

This work was supported by JSPS KAKENHI (Grant number 20K10177) and JST SPRING (Grant Number JPMJSP2138).

First and foremost, I would like to express my deepest gratitude to Professor Hitoshi Niwa, the former Professor of the Department of Dental Anesthesiology, Osaka University Graduate School of Dentistry. Four years ago, he provided me with the invaluable opportunity to pursue my doctoral degree here. His support allowed me to delve into cutting-edge research in natural sciences and brain science, fulfilling my long-cherished dream of entering this fascinating research field.

I am also profoundly grateful to Associate Professor Chiho Kudo. As my academic advisor and defense supervisor, she provided invaluable assistance in refining my dissertation, preparing for my final defense, and facilitating the thesis review process. I am truly grateful for her dedication to my academic development and her willingness to offer advice and encouragement whenever I faced challenges. Without her support, I could not have successfully reached this significant milestone in my academic journey.

My heartfelt appreciation extends to Assistant Professor Shiou-Ling Lu from Department of Oral Cellular Biology, Center for Frontier Oral Science, Osaka University Graduate School of Dentistry. Under her patient instruction, I gained proficiency in using essential research instruments, and she tirelessly addressed my technical questions and uncertainties. Her encouragement and emotional support during moments of doubt gave me the strength to persevere through challenges.

I would like to extend my special thanks to Dr. Nayuka Usami. She played a crucial role in supervising my research, helping me formulate and complete my study, and

guiding me through the experimental methodologies and subsequent thesis revisions. Her mentorship throughout my doctoral journey has been invaluable. I will always hold dear the scientific rigor, truth-seeking spirit, and meticulous work ethic she exemplified, as well as her kindness, humility, and grace towards others. These qualities will continue to inspire and guide me in my future academic and personal endeavors.

I am also deeply grateful to all members of the Department of Dental Anesthesiology. Your selfless support and encouragement have helped me overcome numerous challenges and strengthened my determination to move forward. Here, I not only gained professional knowledge but also experienced the power of teamwork and care. Thank you sincerely for providing indispensable support at every step of my graduate journey.

Thank you all for being part of this incredible journey of my life.

8. References

[1] K. R. Chaudhuri, A. H. Schapira, Non-motor symptoms of Parkinson's disease: Dopaminergic pathophysiology and treatment, Lancet Neurol. 8 (2009) 464–474. https://doi.org/10.1016/S1474-4422(09)70068-7.

[2] J. Jankovic, Parkinson's disease: clinical features and diagnosis, Journal of Neurology, Neurosurgery & Psychiatry 79 (2008) 368–376. https://doi.org/10.1136/jnnp.2007.131045.

[3] G. Wasner, G. Deuschl, Pains in Parkinson disease—many syndromes under one umbrella, Nat Rev Neurol 8 (2012) 284–294. https://doi.org/10.1038/nrneurol.2012.54.

[4] M.A. Lee, R.W. Walker, T.J. Hildreth, W.M. Prentice, A Survey of Pain in Idiopathic Parkinson's Disease, Journal of Pain and Symptom Management 32 (2006) 462–469. https://doi.org/10.1016/j.jpainsymman.2006.05.020.

[5] M.G. Tansey, R.L. Wallings, M.C. Houser, M.K. Herrick, C.E. Keating, V. Joers, Inflammation and immune dysfunction in Parkinson disease, Nat Rev Immunol 22 (2022) 657–673. https://doi.org/10.1038/s41577-022-00684-6.

[6] A. Park, M. Stacy, Non-motor symptoms in Parkinson's disease, J Neurol 256 (2009) 293–298. https://doi.org/10.1007/s00415-009-5240-1.

[7] B. Ford, Pain in Parkinson's disease, Movement Disorders 25 (2010). https://doi.org/10.1002/mds.22716.

[8] C. Cattaneo, W.H. Jost, Pain in Parkinson's Disease: Pathophysiology, Classification and Treatment, J. Integr. Neurosci. 22 (2023) 132. https://doi.org/10.31083/j.jin2205132.

[9] I. Subramanian, J. Farahnik, L.K. Mischley, Synergy of pandemics-social isolation is associated with worsened Parkinson severity and quality of life, Npj Parkinsons Dis. 6 (2020) 28. https://doi.org/10.1038/s41531-020-00128-9.

[10] W. Dieb, O. Ouachikh, F. Durif, A. Hafidi, Lesion of the dopaminergic nigrostriatal pathway induces trigeminal dynamic mechanical allodynia, Brain Behav. 4 (2014) 368–380. https://doi.org/10.1002/brb3.214.

[11] H. Maegawa, Y. Morimoto, C. Kudo, H. Hanamoto, A. Boku, M. Sugimura, T. Kato, A. Yoshida, H. Niwa, Neural mechanism underlying hyperalgesic response to orofacial pain in Parkinson's disease model rats, Neurosci. Res. 96 (2015) 59–68. https://doi.org/10.1016/j.neures.2015.01.006.

[12] H. Maegawa, N. Adachi, H. Hanamoto, C. Kudo, H. Niwa, Bilateral Parkinson's disease model rats exhibit hyperalgesia to subcutaneous formalin administration into the vibrissa pad, PLoS ONE. 14 (2019) e0225928. https://doi.org/10.1371/journal.pone.0225928.

[13] M. G. Tansey, R. L. Wallings, M. C. Houser, M. K. Herrick, C. E. Keating, V. Joers, Inflammation and immune dysfunction in Parkinson disease, Nat. Rev. Immunol. 22 (2022) 657–673. https://doi.org/10.1038/s41577-022-00684-6.

[14] N. Usami, H. Maegawa, M. Hayashi, C. Kudo, H. Niwa, Changes in the analgesic mechanism of oxytocin can contribute to hyperalgesia in Parkinson's disease model rats, PLoS ONE. 19 (2024) e0300081. https://doi.org/10.1371/journal.pone.0300081.

[15] S. Zambito Marsala, M. Tinazzi, R. Vitaliani, S. Recchia, F. Fabris, C. Marchini, A. Fiaschi, G. Moretto, B. Giometto, A. Macerollo, G. Defazio, Spontaneous pain,

pain threshold, and pain tolerance in Parkinson's disease, J Neurol 258 (2011) 627–633. https://doi.org/10.1007/s00415-010-5812-0.

[16] D.E. Jolly, R.B. Paulson, G.W. Paulson, J.A. Pike, Parkinson's disease: a review and recommendations for dental management, Special Care in Dentistry 9 (1989) 74–78. https://doi.org/10.1111/j.1754-4505.1989.tb01032.x.

[17] B. Ford, E.D. Louis, P. Greene, S. Fahn, Oral and genital pain syndromes in Parkinson's disease, Movement Disorders 11 (1996) 421–426. https://doi.org/10.1002/mds.870110411.

[18] T.J. Clifford, M.J. Warsi, C.A. Burnett, P.J. Lamey, Burning mouth in Parkinson's Disease sufferers, Gerodontology 15 (1998) 73–78. https://doi.org/10.1111/j.1741-2358.1998.00073.x.

[19] J. Lipski, R. Nistico, N. Berretta, E. Guatteo, G. Bernardi, N. B. Mercuri, l-DOPA: A scapegoat for accelerated neurodegeneration in Parkinson's disease?, Prog. Neurobiol. 94 (2011) 389–407. https://doi.org/10.1016/j.pneurobio.2011.06.005.

[20] J. W. Wright, J. W. Harding, Importance of the brain angiotensin system in Parkinson's disease, Parkinson's Dis. 2012 (2012) 1–14. https://doi.org/10.1155/2012/860923.

[21] C. Tassorelli, M. Armentero, R. Greco, R. Fancellu, G. Sandrini, G. Nappi, F. Blandini, Behavioral responses and Fos activation following painful stimuli in a rodent model of Parkinson's disease, Brain Res. 1176 (2007) 53–61. https://doi.org/10.1016/j.brainres.2007.08.012.

[22] B. Savić, D. Murphy, N. Japundžić-Žigon, The paraventricular nucleus of the hypothalamus in control of blood pressure and blood pressure variability, Front. Physiol. 13 (2022) 858941. https://doi.org/10.3389/fphys.2022.858941.

[23] J. I. Wamsteeker Cusulin, T. Füzesi, A. G. Watts, J. S. Bains, Characterization of corticotropin-releasing hormone neurons in the paraventricular nucleus of the hypothalamus of Crh-IRES-Cre mutant mice, PLoS ONE. 8 (2013) e64943. https://doi.org/10.1371/journal.pone.0064943.

[24] J. P. Herman, J. G. Tasker, Paraventricular hypothalamic mechanisms of chronic stress adaptation, Front. Endocrinol. 7 (2016). https://doi.org/10.3389/fendo.2016.00137.

[25] S. A. Mousa, P. C. Bopaiah, C. Stein, M. Schäfer, Involvement of corticotropin-releasing hormone receptor subtypes 1 and 2 in peripheral opioid-mediated inhibition of inflammatory pain, Pain. 106 (2003) 297–307. https://doi.org/10.1016/S0304-3959(03)00302-6.

[26] H. Nishino, T. Hashitani, M. Kumazaki, H. Sato, F. Furuyama, Y. Isobe, N. Watari, M. Kanai, S. Shiosaka, Long-term survival of grafted cells, dopamine synthesis/release, synaptic connections, and functional recovery after transplantation of fetal nigral cells in rats with unilateral 6-OHDA lesions in the nigrostriatal dopamine pathway, Brain Res. 534 (1990) 83–93. https://doi.org/10.1016/0006-8993(90)90115-R.

[27] A. Björklund, S. B. Dunnett, The amphetamine induced rotation test: A reassessment of its use as a tool to monitor motor impairment and functional recovery in rodent models of Parkinson's disease, J. Parkinsons Dis. 9 (2019) 17–29. https://doi.org/10.3233/JPD-181525.

[28] S. Jiang, L. Chen, Z.-L. Huang, C.-R. Chen, Role of the paraventricular nucleus of the hypothalamus in sleep–wake regulation, Brain Science Advances 8 (2022) 197–209. https://doi.org/10.26599/BSA.2022.9050017.

[29] S.S. Oh, H.L. Narver, Mouse and Rat Anesthesia and Analgesia, Current Protocols 4 (2024) e995. https://doi.org/10.1002/cpz1.995.

[30] G. Paxinos, C. Watson, The rat brain in stereotaxic coordinates, 6th ed. Cambridge: Elsevier. Academic Press (2007) p. 1.

[31] J. S. Purba, Increased number of vasopressin- and oxytocin-expressing neurons in the paraventricular nucleus of the hypothalamus in depression, Arch. Gen. Psychiatry 53 (1996) 137. https://doi.org/10.1001/archpsyc.1996.01830020055007.

[32] W. R. Lariviere, R. Melzack, The role of corticotropin-releasing factor in pain and analgesia, J. Pain. 84 (2000) 1–12. https://doi.org/10.1016/S0304-3959(99)00193-1.

[33] D. Dubuisson, S.G. Dennis, The formalin test: A quantitative study of the analgesic effects of morphine, meperidine, and brain stem stimulation in rats and cats:, Pain 4 (1977) 161–174. https://doi.org/10.1016/0304-3959(77)90130-0.

[34] A. Tjølsen, O.-G. Berge, S. Hunskaar, J.H. Rosland, K. Hole, The formalin test: an evaluation of the method, Pain 51 (1992) 5–17. https://doi.org/10.1016/0304-3959(92)90003-T.

[35] C.R. McNamara, J. Mandel-Brehm, D.M. Bautista, J. Siemens, K.L. Deranian, M. Zhao, N.J. Hayward, J.A. Chong, D. Julius, M.M. Moran, C.M. Fanger, TRPA1 mediates formalin-induced pain, Proc. Natl. Acad. Sci. U.S.A. 104 (2007) 13525–13530. https://doi.org/10.1073/pnas.0705924104.

[36] A. Siahposht‐Khachaki, P. Pourreza, S. Ezzatpanah, A. Haghparast, Nucleus accumbens dopamine receptors mediate hypothalamus‐induced antinociception in the rat formalin test, European Journal of Pain 21 (2017) 1285‐1294. https://doi.org/10.1002/ejp.1029.

[37] R.A. Domenici, A.C.P. Campos, S.T. Maciel, M.B. Berzuino, M.S. Hernandes, E.T. Fonoff, R.L. Pagano, Parkinson's disease and pain: Modulation of nociceptive circuitry in a rat model of nigrostriatal lesion, Exp. Neurol. 315 (2019) 72–81. https://doi.org/10.1016/j.expneurol.2019.02.007.

[38] C. T. Wotjak, J. Ganster, G. Kohl, F. Holsboer, R. Landgraf, M. Engelmann, Dissociated central and peripheral release of vasopressin, but not oxytocin, in response to repeated swim stress: New insights into the secretory capacities of peptidergic neurons, Neuroscience. 85 (1998) 1209–1222. https://doi.org/10.1016/S0306-4522(97)00683-0.

[39] J. A. Rash, A. Aguirre-Camacho, T. S. Campbell, Oxytocin and pain: A systematic review and synthesis of findings, Clin. J. Pain. 30 (2014) 453–462. https://doi.org/10.1097/AJP.0b013e31829f57df.

[40] P.-E. Juif, P. Poisbeau, Neurohormonal effects of oxytocin and vasopressin receptor agonists on spinal pain processing in male rats, Pain. 154 (2013) 1449–1456. https://doi.org/10.1016/j.pain.2013.05.003.

[41] A. González-Hernández, G. Rojas-Piloni, M. Condés-Lara, Oxytocin and analgesia: Future trends, Trends Pharmacol. Sci. 35 (2014) 549–551. https://doi.org/10.1016/j.tips.2014.09.004.

[42] E.J. Van Bockstaele, B.A.S. Reyes, R.J. Valentino, The locus coeruleus: A key nucleus where stress and opioids intersect to mediate vulnerability to opiate abuse, Brain Res. 1314 (2010) 162–174. https://doi.org/10.1016/j.brainres.2009.09.036.

[43] A. Wyns, J. Hendrix, A. Lahousse, E. De Bruyne, J. Nijs, L. Godderis, A. Polli, The biology of stress intolerance in patients with chronic pain—State of the art and

future directions, J. Clin. Med. 12 (2023) 2245. https://doi.org/10.3390/jcm12062245.

[44] K. Uvnäs-Moberg, M. M. Gross, J. Calleja-Agius, J. D. Turner, The Yin and Yang of the oxytocin and stress systems: Opposites, yet interdependent and intertwined determinants of lifelong health trajectories, Front. Endocrinol. 15 (2024) 1272270. https://doi.org/10.3389/fendo.2024.1272270.

[45] J. P. Herman, J. M. McKlveen, S. Ghosal, B. Kopp, A. Wulsin, R. Makinson, J. Scheimann, B. Myers, Regulation of the hypothalamic‐pituitary‐adrenocortical stress response, in: Y.S. Prakash (Ed.), Comprehensive Physiology, 1st ed., Wiley, 2016: pp. 603‐621. https://doi.org/10.1002/cphy.c150015.

[46] W. D. Willis, K. N. Westlund, Neuroanatomy of the pain system and of the pathways that modulate pain, J. Neurophysiol. 14 (1997) 2–31. https://doi.org/10.1097/00004691-199701000-00002.

[47] L. Rinaman, Hindbrain noradrenergic A2 neurons: Diverse roles in autonomic, endocrine, cognitive, and behavioral functions, American Journal of Physiology-Regulatory, Integrative and Comparative Physiology. 300 (2011) R222–R235. https://doi.org/10.1152/ajpregu.00556.2010.

[48] T. Onaka, T. Yamashita, X. Liu, K. Honda, T. Saito, K. Yagi, Medullary A1 noradrenergic neurons may mediate oxytocin release after noxious stimuli, Neuroreport. 12 (2001) 2499–2502. https://doi.org/10.1097/00001756-200108080-00042.

[49] T. Onaka, J. R. Palmer, K. Yagi, A selective role of brainstem noradrenergic neurons in oxytocin release from the neurohypophysis following noxious stimuli in the rat, Neurosci. Res. 25 (1996) 67–75. https://doi.org/10.1016/0168-0102(96)01029-2.

[50] C. E. Snyder, Y. Silberman, Corticotropin releasing factor and norepinephrine related circuitry changes in the bed nucleus of the stria terminalis in stress and alcohol and substance use disorders, Neuropharmacology. 201 (2021) 108814. https://doi.org/10.1016/j.neuropharm.2021.108814.

[51] A.E. Snyder, Y. Silberman, Corticotropin releasing factor and norepinephrine related circuitry changes in the bed nucleus of the stria terminalis in stress and alcohol and substance use disorders, Neuropharmacology 201 (2021) 108814. https://doi.org/10.1016/j.neuropharm.2021.108814.

[52] M. J. Brownstein, J. T. Russell, H. Gainer, Synthesis, transport, and release of posterior pituitary hormones, Sciences. 207 (1980) 373–378. https://doi.org/10.1126/science.6153132.

[53] Y. Meguro, K. Miyano, S. Hirayama, Y. Yoshida, N. Ishibashi, T. Ogino, Y. Fujii, S. Manabe, M. Eto, M. Nonaka, H. Fujii, Y. Ueta, M. Narita, N. Sata, T. Yada, Y. Uezono, Neuropeptide oxytocin enhances μ opioid receptor signaling as a positive allosteric modulator, J. Pharmacol. Sci. 137 (2018) 67–75. https://doi.org/10.1016/j.jphs.2018.04.002.

[54] N. Burford, N. Webster, D. Cruz-Topete, hypothalamic-pituitary-adrenal axis modulation of glucocorticoids in the cardiovascular system, Int. J. Mol. Sci. 18 (2017) 2150. https://doi.org/10.3390/ijms18102150.

[55] C. Rivier, W. Vale, Modulation of stress-induced ACTH release by corticotropin-releasing factor, catecholamines and vasopressin, Nature. 305 (1983) 325–327. https://doi.org/10.1038/305325a0.

[56] G. Aguilera, Y. Liu, The molecular physiology of CRH neurons, Front. Neuroendocrinol. 33 (2012) 67–84. https://doi.org/10.1016/j.yfrne.2011.08.002.

[57] Y. M. Ulrich-Lai, J. P. Herman, Neural regulation of endocrine and autonomic stress responses, Nat. Rev. Neurosci. 10 (2009) 397–409. https://doi.org/10.1038/nrn2647.

[58] J. Cui, D. Zhao, M. Xu, Z. Li, J. Qian, N. Song, J. Wang, J. Xie, Characterization of graded 6-Hydroxydopamine unilateral lesion in medial forebrain bundle of mice, Sci. Rep. 14 (2024) 3721. https://doi.org/10.1038/s41598-024-54066-0.

[59] K. Kamińska, T. Lenda, J. Konieczny, A. Czarnecka, E. Lorenc-Koci, Depressive-like neurochemical and behavioral markers of Parkinson's disease after 6-OHDA administered unilaterally to the rat medial forebrain bundle, Pharmacol. Rep. 69 (2017) 985–994. https://doi.org/10.1016/j.pharep.2017.05.016.

[60] A.J. Espay, P.A. LeWitt, H. Kaufmann, Norepinephrine deficiency in Parkinson's disease: The case for noradrenergic enhancement, Movement Disorders 29 (2014) 1710–1719. https://doi.org/10.1002/mds.26048.

[61] C.-L. Huang, F. Liu, Y.-Y. Zhang, J. Lin, M. Fu, Y.-L. Li, C. Zhou, C.-J. Li, J.-F. Shen, Activation of oxytocin receptor in the trigeminal ganglion attenuates orofacial ectopic pain attributed to inferior alveolar nerve injury, J. Neurophysiol. 125 (2021) 223–231. https://doi.org/10.1152/jn.00646.2020.

[62] E. García-Boll, G. Martínez-Lorenzana, M. Condés-Lara, A. González-Hernández, Oxytocin inhibits the rat medullary dorsal horn Sp5c/C1 nociceptive transmission through OT but not V 1A receptors, Neuropharmacology. 129 (2018) 109–117. https://doi.org/10.1016/j.neuropharm.2017.11.031.

[63] S. Hobo, K. Hayashida, J. C. Eisenach, Oxytocin inhibits the membrane depolarization-induced increase in intracellular calcium in capsaicin sensitive

sensory neurons: A peripheral mechanism of analgesic action, Anesth. Anal. 114 (2012) 442–449. https://doi.org/10.1213/ANE.0b013e31823b1bc8.

[64] A. M. Harriott, M. Kaya, C. Ayata, Oxytocin shortens spreading depolarization-induced periorbital allodynia, J. Headache Pain 25 (2024) 152. https://doi.org/10.1186/s10194-024-01855-7.

[65] Y. F. Liang, X. Q. Chen, M. T. Zhang, H. Y. Tang, G. M. Shen, Research progress of central and peripheral corticotropin-releasing hormone in irritable bowel syndrome with comorbid dysthymic disorders, Gut Liver. 18 (2024) 391–403. https://doi.org/10.5009/gnl220346.

[66] K. L. Brunson, D. E. Grigoriadis, M. T. Lorang, T. Z. Baram, Corticotropin-Releasing hormone (CRH) downregulates the function of its receptor (CRF1) and induces CRF1 expression in hippocampal and cortical regions of the immature rat brain, Exp. Neurol. 176 (2002) 75–86. https://doi.org/10.1006/exnr.2002.7937.

[67] H. Guo, H. Lai, B. Long, L. Xu, E.H.C. Wang, J. Shapiro, K.J. McElwee, Increased CRHR1 expression on monocytes from patients with AA enables a pro-inflammatory response to corticotrophin-releasing hormone, Exp. Dermatol. 33 (2024) e15182. https://doi.org/10.1111/exd.15182.

[68] S. A. Mousa, B. I. Khalefa, M. Shaqura, M. Al-Madol, S. Treskatsch, M. Schäfer, Superior control of inflammatory pain by corticotropin-releasing factor receptor 1 via opioid peptides in distinct pain-relevant brain areas, J. Neuroinflamm. 19 (2022) 148. https://doi.org/10.1186/s12974-022-02498-8.

[69] A. Batla, V. Phé, L. De Min, J. N. Panicker, Nocturia in Parkinson's disease: Why does it occur and how to manage?, Movement Disord. Clin. Pract. 3 (2016) 443–451. https://doi.org/10.1002/mdc3.12374.

[70] L. Yeo, R. Singh, M. Gundeti, J. M. Barua, J. Masood, Urinary tract dysfunction in Parkinson's disease: A review, Int. Urol. Nephrol. 44 (2012) 415–424. https://doi.org/10.1007/s11255-011-9969-y.

[71] K. Csabafi, K. E. Ibos, É. Bodnár, K. Filkor, J. Szakács, Z. Bagosi, A brain region-dependent alteration in the expression of vasopressin, corticotropin-releasing factor, and their receptors might be the background of kisspeptin-13-induced hypothalamic-pituitary-adrenal axis activation and anxiety in rats, Biomedicines 11 (2023) 2446. https://doi.org/10.3390/biomedicines11092446.

[72] C. Buhmann, N. Wrobel, W. Grashorn, O. Fruendt, K. Wesemann, S. Diedrich, U. Bingel, Pain in Parkinson disease: A cross-sectional survey of its prevalence, specifics, and therapy, J. Neurol. 264 (2017) 758–769. https://doi.org/10.1007/s00415-017-8426-y.

[73] N. P. Quinn, A. E. Lang, W. C. Koller, C. D. Marsden, Painful Parkinson's disease, Lancet. 327 (1986) 1366–1369. https://doi.org/10.1016/S0140-6736(86)91674-0.

[74] A. Nebe, G. Ebersbach, Pain intensity on and off levodopa in patients with Parkinson's disease, Mov. Disord. 24 (2009) 1233–1237. https://doi.org/10.1002/mds.22546.

[75] M.A.S. Zella, C. May, T. Müller, M. Ahrens, L. Tönges, R. Gold, K. Marcus, D. Woitalla, Landscape of pain in Parkinson's disease: Impact of gender differences, Neurol. Res. 41 (2019) 87–97. https://doi.org/10.1080/01616412.2018.1531208.

[76] J. E. Quintero, D. J. Dooley, F. Pomerleau, P. Huettl, G. A. Gerhardt, Amperometric measurement of glutamate release modulation by gabapentin and pregabalin in rat neocortical slices: Role of voltage-sensitive Ca2+ α2 δ-1 subunit, J. Pharmacol. Exp. Ther. 338 (2011) 240–245. https://doi.org/10.1124/jpet.110.178384.

9. Figures

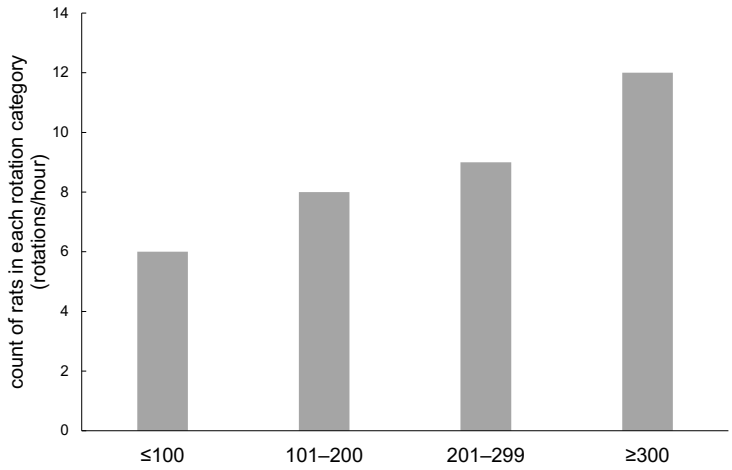

Fig. 1. Distribution of rotational behavior in 6-OHDA-injected rats.
The distribution of rotational behavior in 35 6-OHDA-injected rats. The rats were categorized into four groups based on the number of rotations per hour.

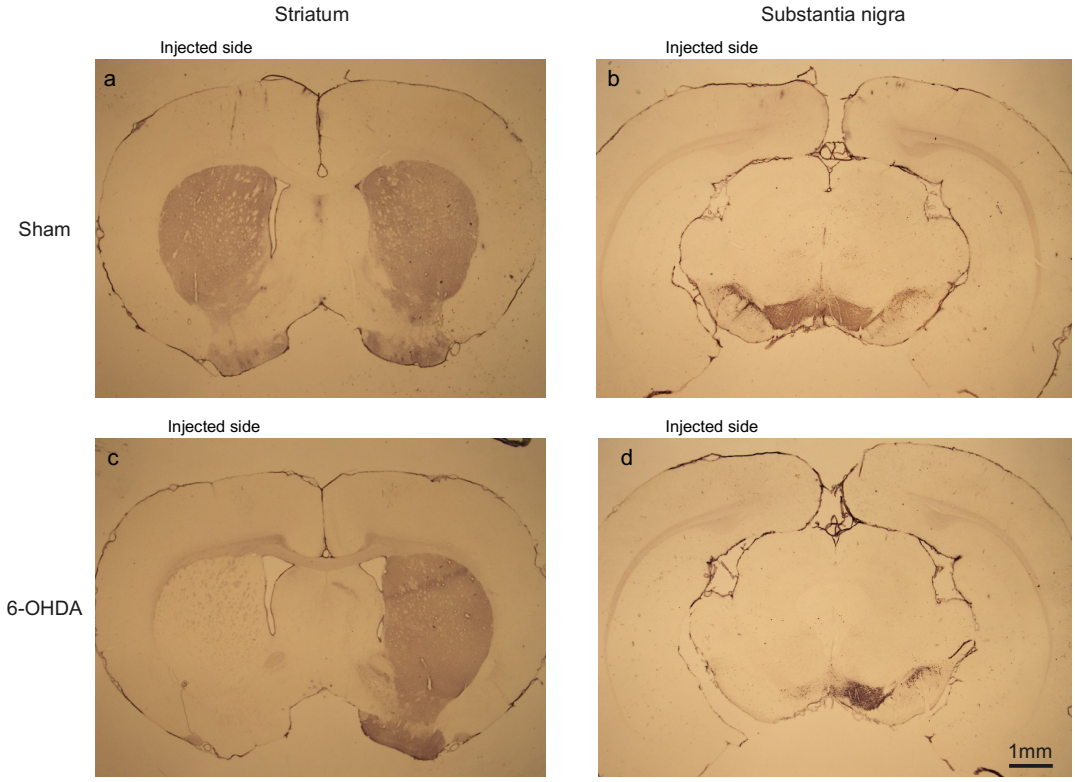

Fig. 2. Tyrosine Hydroxylase (TH) Immunoreactivity Following 6-Hydroxydopamine (6-OHDA) Injection.
(a, b) No alterations in TH immunoreactivity were observed in the striatum and substantia nigra on the saline-injected side.
(c, d) A reduction in TH immunoreactivity was detected in the striatum and substantia nigra on the 6-OHDA-injected side.

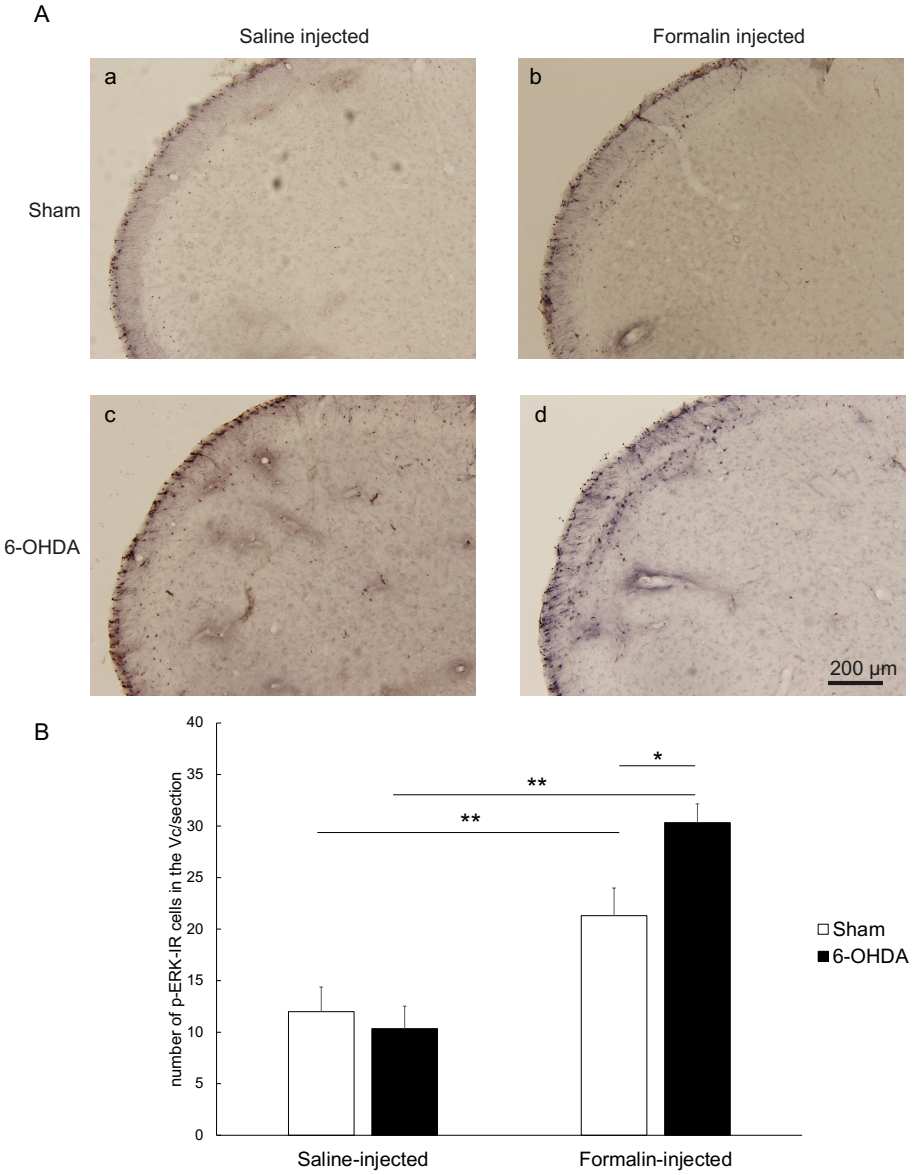

Fig. 3. p-ERK Immunoreactivity in the Trigeminal Spinal Subnucleus Caudalis Following Formalin Injection.
(A) Photomicrographs of p-ERK immunohistochemical staining in the trigeminal spinal subnucleus caudalis:
(a, c) Saline-injected group; (b, d) Formalin-injected group.
(B) In the formalin-injected group, the number of p-ERK-immunoreactive (-IR) cells was significantly higher in 6-OHDA rats compared to sham rats.
**p-value* < 0.05. ***p-value* < 0.01.

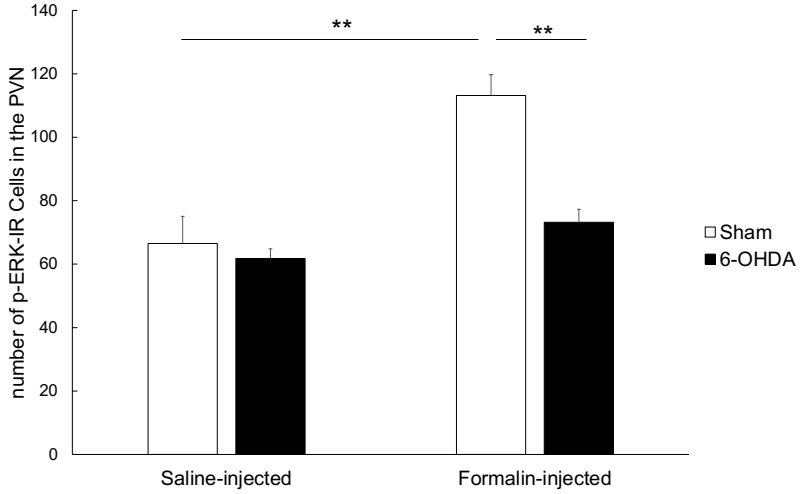

Fig. 4. Number of p-ERK-IR cells in the PVN by double immunofluorescence with p-ERK and oxytocin (OXT), corticotropin-releasing hormone (CRH), vasopressin (AVP) .
The number of p-ERK-IR cells was quantified in sections used for evaluating OXT (Fig. 4), CRH (Fig. 5), and AVP (Fig. 6) across four experimental groups: Sham rats with saline injection group, Sham rats with formalin injection group, 6-OHDA rats with saline injection group, and 6-OHDA rats with formalin injection group.* *p-value* < 0.01

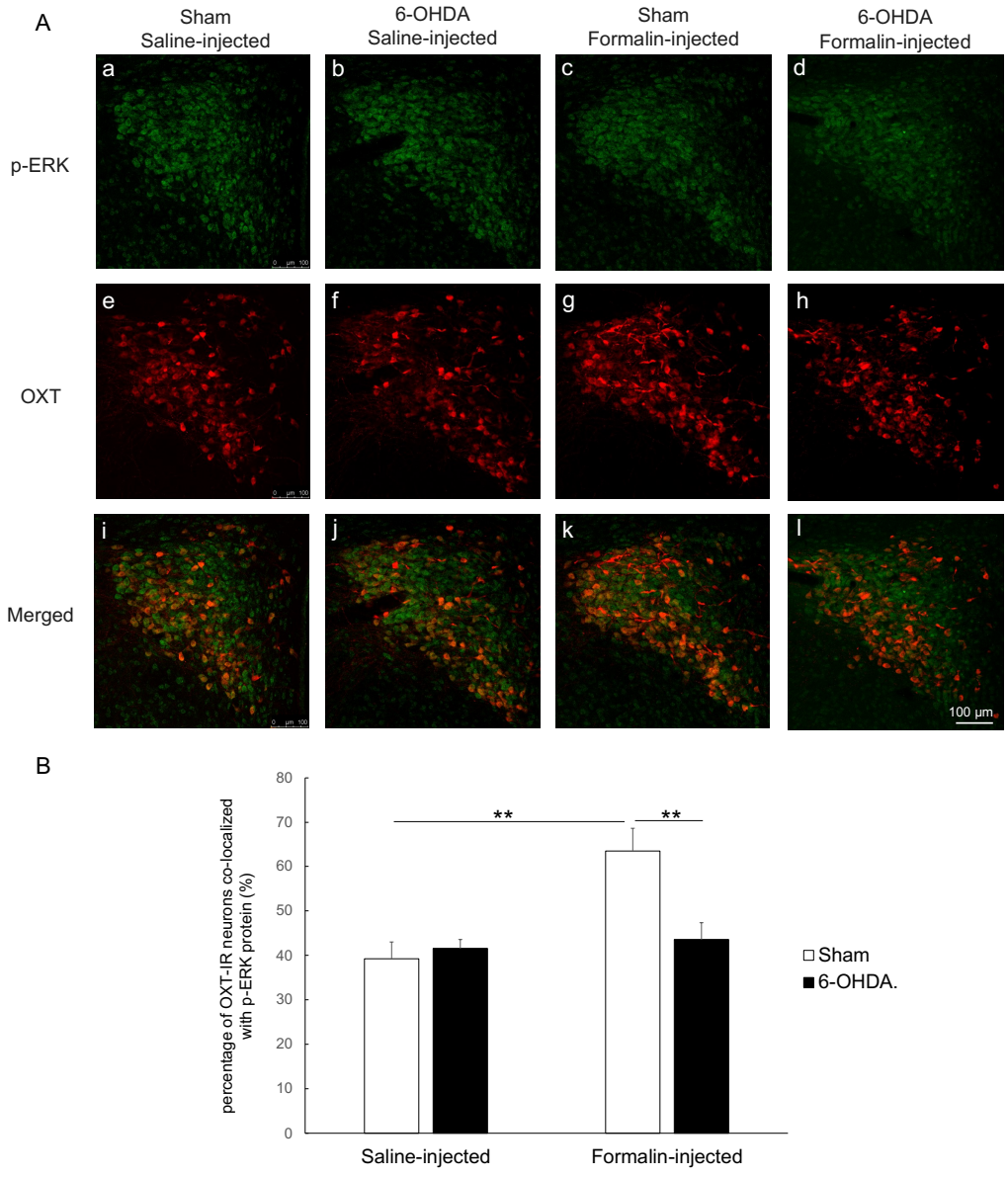

Fig. 5. Co-expression of p-ERK and OXT-IR cells in the PVN.
(A) Photomicrographs of p-ERK-IR cells (a–d), OXT-IR cells (e–h), and merged images (i–l).
(B) Changes in the percentage of OXT-IR neurons co-localized with p-ERK protein.
***p-value* < 0.01.

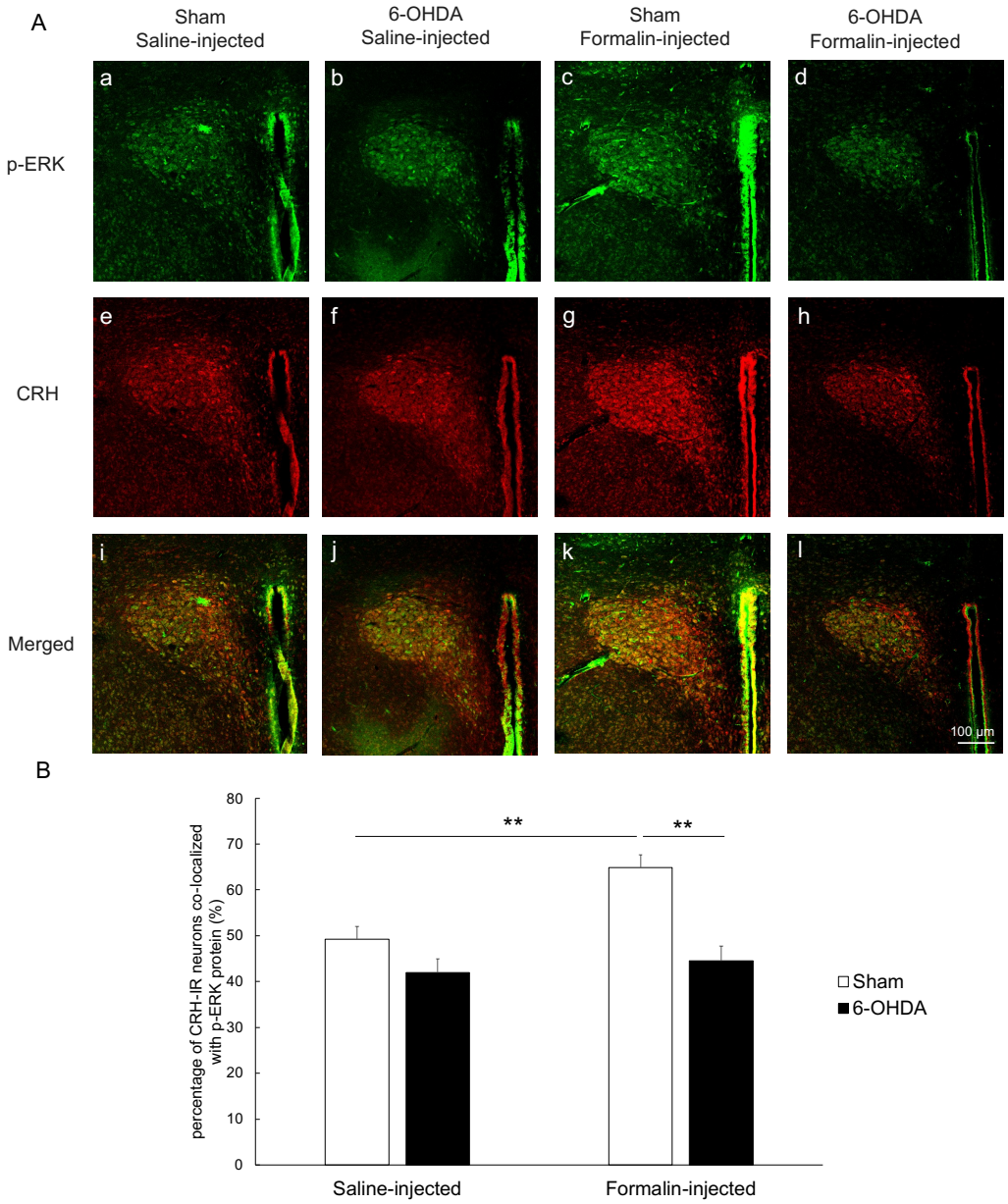

Fig. 6. Co-expression of p-ERK and CRH-IR cells in the PVN.
(A) Photomicrographs of p-ERK-IR cells (a–d), CRH-IR cells (e–h), and merged images (i–l).
(B) Changes in the percentage of CRH-IR neurons co-localized with p-ERK protein.
***p-value* < 0.01.

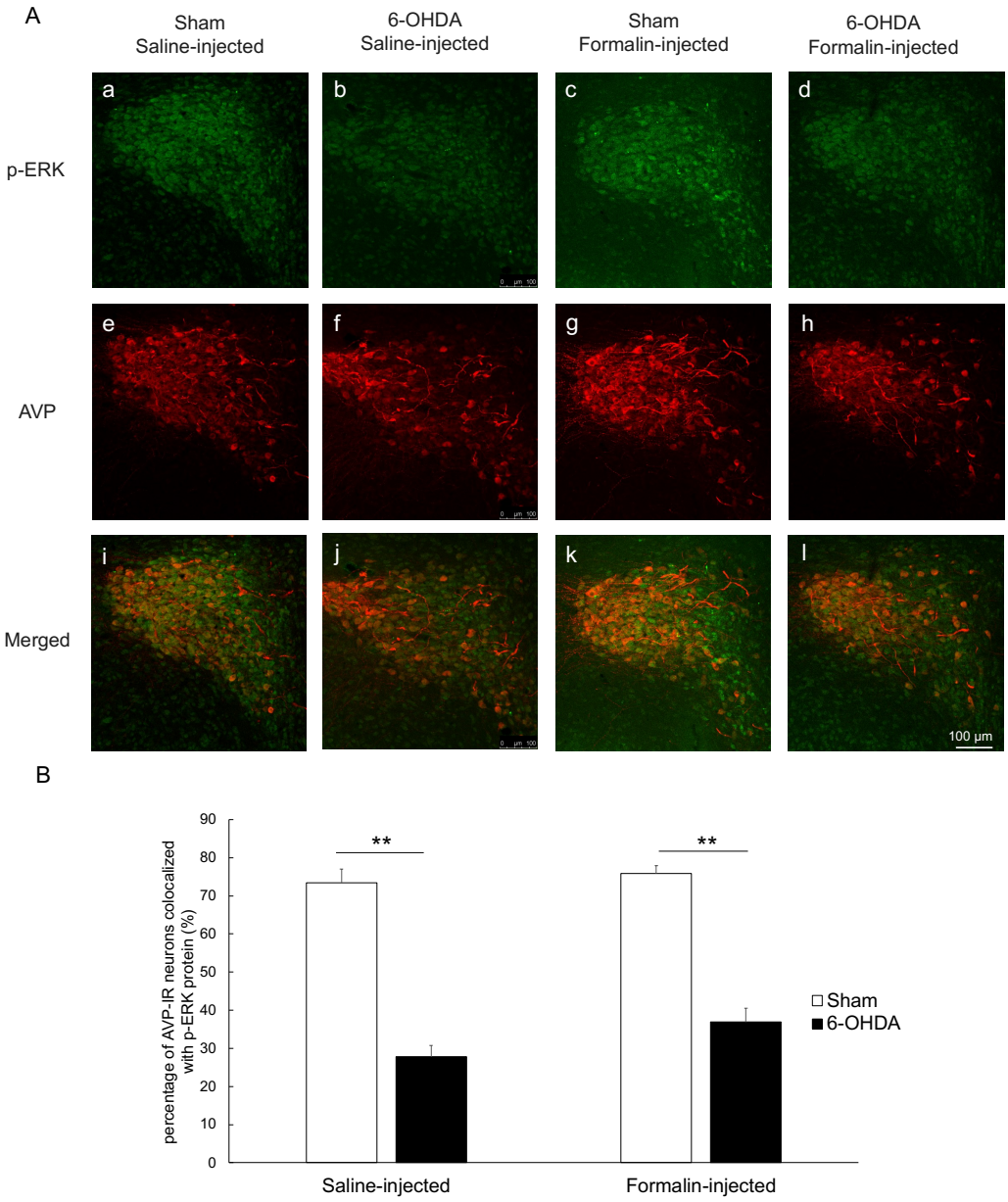

Fig. 7. Co-expression of p-ERK and AVP-IR cells in the PVN.
(A) Photomicrographs of p-ERK-IR cells (a–d), AVP-IR cells (e–h), and merged images (i–l).
(B) Changes in the percentage of AVP-IR neurons co-localized with p-ERK protein.
***p-value* < 0.01.

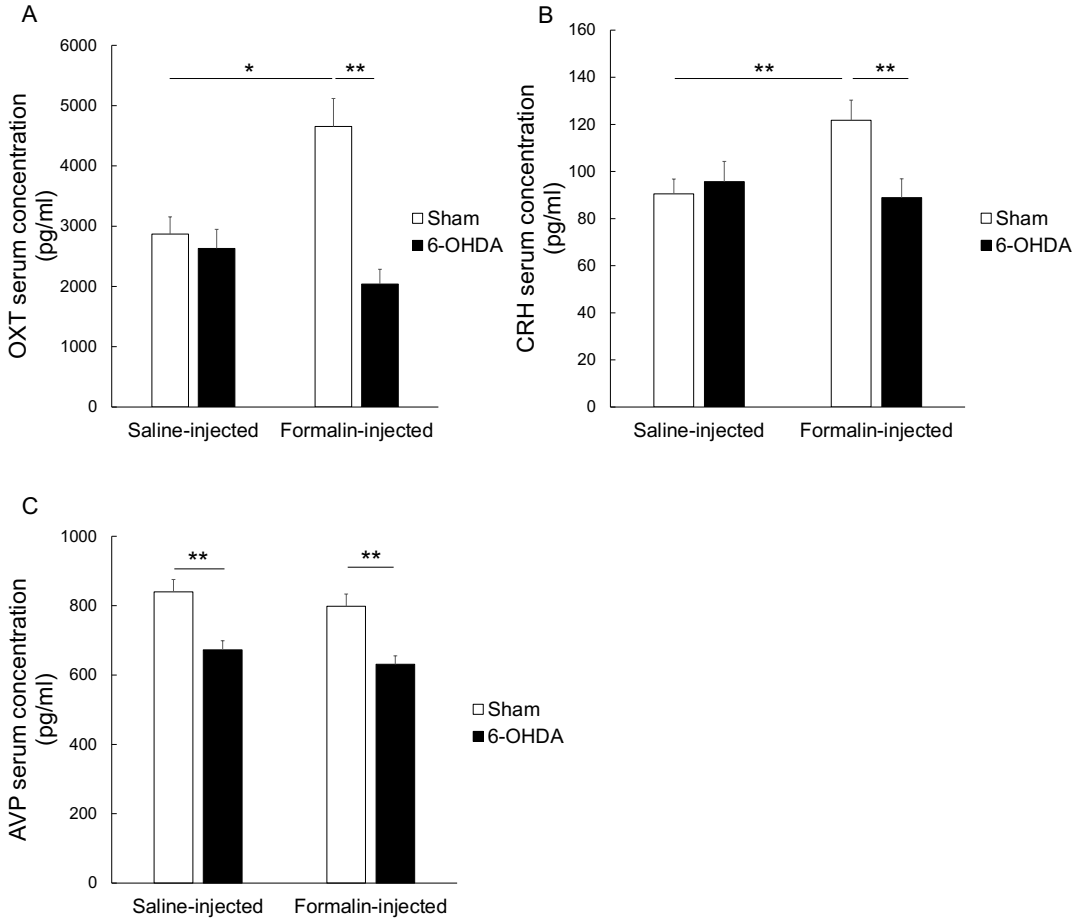

Fig. 8. Changes in the serum OXT, AVP, and CRH concentrations.
(A) OXT: Formalin injection significantly increased OXT concentration in sham rats but had no effect in 6-OHDA rats. The OXT concentration was lower in formalin-injected 6-OHDA rats compared to formalin-injected sham rats.
(B) CRH: Formalin injection significantly increased CRH concentration in sham rats, but no change was observed in 6-OHDA rats. CRH levels were lower in formalin-injected 6-OHDA rats compared to formalin-injected sham rats.
(C) AVP: Serum AVP concentration was significantly lower in 6-OHDA rats compared to sham rats, regardless of formalin or saline injection.* p-value < 0.05, **p-value < 0.01.